

Sweet spot in the RuCl_3 magnetic system: nearly ideal $j_{\text{eff}}=1/2$ moments and maximized K/J ratio under pressure

Pritam Bhattacharyya and Liviu Hozoi

Institute for Theoretical Solid State Physics, Leibniz IFW Dresden, Helmholtzstraße 20, 01069 Dresden, Germany

Quirin Stahl

Institut für Festkörper- und Materialphysik, Technische Universität Dresden, 01062 Dresden, Germany

Jochen Geck

*Institut für Festkörper- und Materialphysik, Technische Universität Dresden, 01062 Dresden, Germany and
Würzburg-Dresden Cluster of Excellence *ct.qmat*,
Technische Universität Dresden, 01062 Dresden, Germany*

Nikolay A. Bogdanov

Max Planck Institute for Solid State Research, Heisenbergstraße 1, 70569 Stuttgart, Germany

(Dated: February 2, 2023)

Maximizing the ratio between Kitaev and residual Heisenberg interactions is a major goal in nowadays research on Kitaev-Heisenberg quantum magnets. Here we investigate Kitaev-Heisenberg exchange in a recently discovered crystalline phase of RuCl_3 under pressure — it displays unusually high symmetry, with only one type of Ru-Ru links, and uniform Ru-Cl-Ru bond angles of $\approx 93^\circ$. By quantum chemical calculations in this particular honeycomb-lattice setting we find a very small J , which yields a K/J ratio as large as ~ 100 . Interestingly, we also find that this is associated with vanishingly small d -shell trigonal splittings, i.e., minimal departure from ideal $j_{\text{eff}}=1/2$ moments. This reconfirms RuCl_3 as a most promising platform for materializing the much sought-after Kitaev spin-liquid phase and stimulates further experiments under strain and pressure.

Introduction. Sizable, bond-dependent Kitaev interactions [1, 2] have been confirmed by now in several honeycomb transition-metal (TM) oxides and halides. The magnetic ground state however is in most of these systems ordered, due to residual isotropic Heisenberg couplings, both nearest- [3, 4] and farther-neighbor. A main question is therefore which is the most suited chemical platform and set of structural parameters (e.g., bond lengths and bond angles) maximizing the ratio between Kitaev and Heisenberg exchange.

A distinct system in this context is RuCl_3 — although it is ordered antiferromagnetically under normal conditions, this antiferromagnetic phase lies in close proximity to the quantum spin liquid [5]. In particular, the latter can be reached by applying a modest in-plane magnetic field [6–8], which raises the question if strain or pressure could be used as well for tuning the magnetic ground state. Interestingly, a new crystalline phase has been recently identified under pressure of 1.26 GPa [9]. Here we report *ab initio* quantum chemical results for the Ru-site multiplet structure and effective intersite couplings in this recently discovered crystalline arrangement. The computations reveal an unusually large K/J ratio of ~ 100 , reconfirming RuCl_3 as one of the most promising chemical settings for materializing the Kitaev spin-liquid ground state. Additionally, we find a very peculiar inner structure of the effective moments, with d -shell trigonal crystal-field splittings as low as 9 meV, 4–5 times less than in RuCl_3 under ambient pressure [10–13]. This

points to minimal departure from ideal $j_{\text{eff}}=1/2$ moments [2, 14], through near cancellation of two different effects — trigonal compression of the ligand cage and anisotropic fields related to farther ions. The apparent correlation between minimal departure from ideal, cubic-symmetry $j_{\text{eff}}=1/2$ moments and maximized K/J ratio is quite remarkable. It seems to indicate that the nearest-neighbor J is minimized in the case of degenerate t_{2g} orbitals.

Ru-site multiplet structure. The octahedral-cage ligand field splits the Ru $4d$ levels into e_g and t_{2g} components, with the latter lying at significantly lower energy; the large $t_{2g}-e_g$ splitting yields then a t_{2g}^5 leading ground-state configuration. With one hole ($s=1/2$) in the t_{2g} sector ($l_{\text{eff}}=1$), sizable spin-orbit coupling (SOC) provides a set of fully occupied $j_{\text{eff}}=3/2$ and magnetically active $j_{\text{eff}}=1/2$ states. For three-fold [9] (or lower) site symmetry, the degeneracy of the t_{2g} sublevels is typically lifted and the $j_{\text{eff}}=1/2$ and $j_{\text{eff}}=3/2$ spin-orbit states may feature some degree of admixture. To determine the $\text{Ru}^{3+} 4d^5$ multiplet structure in $\alpha\text{-RuCl}_3$ at $p=1.26$ GPa, we carried out quantum chemical computations using the MOLPRO suite of programs [15] and crystallographic data as reported by Stahl *et al.* [9]. A cluster consisting of one ‘central’ RuCl_6 octahedron and the three in-plane adjacent octahedra was designed for this purpose. The crystalline environment was modeled as a large array of point charges which reproduces the Madelung field within the cluster volume; to generate this point-charge embedding

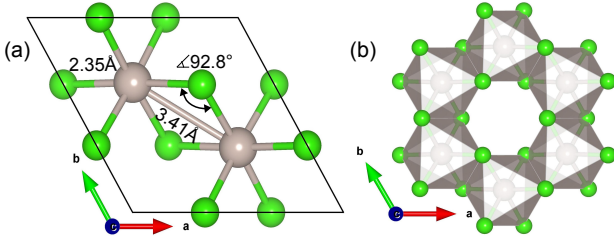


FIG. 1. (a) Unit cell of α -RuCl₃ for $p = 1.26$ GPa [9]. (b) Hexagonal ring of edge-sharing RuCl₆ octahedra. Grey and green spheres represent Ru and Cl ions, respectively.

we employed the EWALD program [16, 17]. The numerical investigation was initiated as a complete active space self-consistent field (CASSCF) calculation [18, 19] with all five $4d$ orbitals of the central Ru ion considered in the active orbital space. Post-CASSCF correlation computations were carried out at the level of multireference configuration-interaction (MRCI) with single and double excitations [18, 20] out of the Ru $4d$ and Cl $3p$ orbitals of the central RuCl₆ octahedron. SOC was accounted for following the procedure described in Ref. [21] [22].

The Ru³⁺ $4d^5$ multiplet structure in the newly discovered crystalline phase of α -RuCl₃ is depicted in Table I, at three different levels of approximation: CASSCF, MRCI, and MRCI+SOC. This allows to easily disentangle three different effects: crystal-field splittings, post-CASSCF correlation-induced corrections, and of spin-orbit interactions. As concerns the former, we find that the trigonal splitting within the t_{2g} levels is tiny, 9 meV, 4–5 times smaller than in α -RuCl₃ at ambient pressure [10–13]. Having nearly degenerate t_{2g} levels for sizable amount of trigonal distortion of the ligand cage sounds odd at first. What makes it happen is the presence of a competing effect — trigonal fields related to the anisotropy of the extended solid-state environment. Mutual cancellation of those two yields cubic-like Ru-site multiplet structure. Quite evident in Table I is also the presence of minimal splittings within the $j_{\text{eff}} = 3/2$ -like manifold once SOC is accounted for (last column), i.e., minimal admixture of $j_{\text{eff}} = 1/2$ and $j_{\text{eff}} = 3/2$ spin-orbit states.

It is additionally seen that the post-CASSCF MRCI treatment yields sizable corrections to some of the relative energies, the most substantial arising for the $^6A_{1g}$ crystal-field term.

Intersite magnetic couplings for proximate $j_{\text{eff}} = 1/2$ moments. To obtain the intersite effective magnetic couplings, a cluster with two edge-sharing RuCl₆ octahedra in the central region was considered. The four in-plane RuCl₆ octahedra coordinating this two-octahedra central unit were also explicitly included in the quantum chemical computations but using more compact basis sets [23]. CASSCF computations were carried out with six (Ru t_{2g}) valence orbitals and ten electrons as active (ab-

breviated as (10e,6o) active space) [24]. Subsequently, three other types of wave-functions were generated, using in each case the orbitals obtained from the (10e,6o) CASSCF calculation: (i) single-configuration (SC) $t_{2g}^5 - t_{2g}^6$ (i.e., the $t_{2g}^4 - t_{2g}^6$ and $t_{2g}^6 - t_{2g}^4$ configurations which were accounted for in the initial (10e,6o) CASSCF were excluded in this case by imposing appropriate orbital-occupation restrictions), (ii) (22e,12o) complete active space configuration-interaction (CASSCF) wave-functions, as full configuration-interaction expansions within the space defined by the Ru t_{2g} and bridging-Cl $3p$ orbitals, and (iii) MRCI wave-functions having the (10e,6o) CASSCF as kernel and accounting for single and double excitations out of the central-unit Ru t_{2g} and bridging-Cl $3p$ orbitals. By comparing data at these different levels of approximation, it is possible to draw conclusions on the role of various (super)exchange mechanisms.

The CASSCF optimization was performed for the lowest nine singlet and lowest nine triplet states associated with the (10e,6o) setting. Those were the states for which SOC was further accounted for [21], either at SC, CASSCF, CASSCF, or MRCI level, which yields in each case a number of 36 spin-orbit states.

Only one type of Ru-Ru link is present in α -RuCl₃ at $p = 1.26$ GPa. A unit of two nearest-neighbor octahedra exhibits C_{2h} point-group symmetry, implying a generalized bilinear effective spin Hamiltonian of the following form for a pair of adjacent $1/2$ -pseudospins $\tilde{\mathbf{S}}_i$ and $\tilde{\mathbf{S}}_j$:

$$\mathcal{H}_{ij}^{(\gamma)} = J\tilde{\mathbf{S}}_i \cdot \tilde{\mathbf{S}}_j + K\tilde{S}_i^\gamma \tilde{S}_j^\gamma + \sum_{\alpha \neq \beta} \Gamma_{\alpha\beta}(\tilde{S}_i^\alpha \tilde{S}_j^\beta + \tilde{S}_i^\beta \tilde{S}_j^\alpha). \quad (1)$$

The $\Gamma_{\alpha\beta}$ coefficients denote the off-diagonal components of the 3×3 symmetric-anisotropy exchange matrix; $\alpha, \beta, \gamma \in \{x, y, z\}$. An antisymmetric Dzyaloshinskii-

TABLE I. Ru³⁺ $4d^5$ multiplet structure; all five $4d$ orbitals were considered in the active space. Each value in the MRCI+SOC column indicates a Kramers doublet (KD); for each of the $t_{2g}^4 e_g^1$ crystal-field terms, only the lowest and highest KDs are shown. Only the crystal-field terms enlisted in the table were included in the spin-orbit computation. Notations corresponding to O_h symmetry are used.

Ru ³⁺ $4d^5$ splittings (eV)	CASSCF	MRCI	MRCI +SOC
$^2T_{2g} (t_{2g}^5)$	0	0	0
	0.01	0.01	0.19
	0.01	0.01	0.20
$^4T_{1g} (t_{2g}^4 e_g^1)$	1.16	1.32	1.38
	1.17	1.32	
	1.17	1.32	1.49
$^6A_{1g} (t_{2g}^3 e_g^2)$	1.15	1.59	1.78 ($\times 3$)
$^4T_{2g} (t_{2g}^4 e_g^1)$	1.84	1.93	2.06
	1.85	1.94	
	1.85	1.94	2.11

Moriya coupling is not allowed, given the inversion center.

The lowest four spin-orbit eigenstates from the MOLPRO output (eigenvalues lower by ~ 0.2 eV with respect to the eigenvalues of higher-lying excited states, as illustrated for example in Table I) were mapped onto the eigenvectors of the effective spin Hamiltonian (1), following the procedure described in Refs. [10, 25]: those four expectation values and the matrix elements of the Zeeman Hamiltonian in the basis of the four lowest-energy spin-orbit eigenvectors are put in direct correspondence with the respective eigenvalues and matrix elements of (1). Having two of the states in the same irreducible representation of the C_{2h} point group, such one-to-one mapping translates into two possible sets of effective magnetic couplings. The relevant array is chosen as the one whose g factors fit the g factors corresponding to a single $\text{RuCl}_6 t_{2g}^5$ octahedron. We used the standard coordinate frame usually employed in the literature, different from the rotated frame employed in earlier quantum chemical studies [10, 26, 27] that affects the sign of Γ (see also discussion in [28]).

Nearest-neighbor effective magnetic couplings as obtained at four different levels of theory (SOC included) are depicted in Table II. The most remarkable finding is the vanishingly small J value in the spin-orbit MRCI computations, which yields a K - Γ - Γ' effective spin model for the nearest-neighbor magnetic interactions. That this coincides with realizing nearly ideal $j_{\text{eff}} = 1/2$ moments at the TM sites seems to be more than merely fortuitous, see also discussion in the next section.

The competition between ligand and ‘crystal’ trigonal fields (i.e., between nearest-neighbor and beyond-nearest-neighbor electrostatics) and possible important implications as concerns the overall magnetic properties of a given system have been earlier discussed in relation to single-site effective magnetic parameters such as the single-ion anisotropy [29] — in particular, it is in principle possible to revert the sign of the latter by modifying the amount of ligand-cage trigonal distortion [29]. Finding that this applies as well to intersite effective interaction parameters (i.e., the Heisenberg J) is novel.

For comparison, the MRCI nearest-neighbor couplings in RuCl_3 at ambient pressure are $K = -5.6$, $J = 1.2$, $\Gamma = 1.2$, and $\Gamma' = -0.7$ (meV) [10]. The Heisenberg J being sizable at ambient pressure, the K/J ratio is much smaller than for the set of parameters provided in Table II. This is realized for somewhat stronger trigonal compression of the Cl_6 polyhedron and additional small distortions that actually lower the Ru-site point-group symmetry to less than trigonal.

Also notable is the fact that K is basically the same at three different levels of approximation (first column in Table II): SC (only the $t_{2g}^5 - t_{2g}^5$ electron configuration considered), CASSCF (10e,6o) ($t_{2g}^5 - t_{2g}^5$ and $t_{2g}^4 - t_{2g}^6$ configurations treated on the same footing), and CASCI

TABLE II. Nearest-neighbor magnetic couplings (meV), results of spin-orbit calculations at various levels of theory. CASCI (22e,12o) stands for a full configuration-interaction within the space defined by the Ru t_{2g} and bridging-Cl $3p$ orbitals. The MRCI is performed having the (10e,6o) CASSCF wave-function as kernel.

	K	J	$\Gamma_{xy} \equiv \Gamma$	$\Gamma_{yz} = \Gamma_{zx} \equiv \Gamma'$
SC	-1.75	0.35	-0.11	0.42
CASSCF (10e,6o)	-1.73	-1.04	0.89	0.46
CASCI (22e,12o)	-1.72	-1.04	0.89	0.47
MRCI	-3.73	-0.03	1.62	0.45

(22e,12o) (also excitations from the bridging-Cl $3p$ to TM t_{2g} orbitals taken into account). It indicates that intersite TM $t_{2g} \rightarrow \text{TM } t_{2g}$ and ligand $2p \rightarrow \text{TM } t_{2g}$ excitations do not affect K . What matters as concerns the size of the Kitaev coupling K are (i) direct exchange, with a contribution of -1.75 meV, and (ii) excitations to higher-lying states and so called dynamical correlation effects accounted for in MRCI, with a contribution of -2 meV.

Anisotropic direct exchange as found in the SC calculation represents very interesting new physics, not addressed so far in the literature. Finding that nearly 50% of the Kitaev effective coupling constant K has to do with direct exchange and that the off-diagonal anisotropic coupling Γ' , which may give rise to spin-liquid ground states by itself [30], comes $\sim 100\%$ from direct exchange (last column in Table II) obviously challenges present views and notions in Kitaev-Heisenberg quantum magnetism research and superexchange theory. To provide additional reference points, we computed the isotropic direct exchange contribution [31] for holes in plaquette-plane TM orbitals having overlapping lobes along the Ru-Ru axis: this amounts to 25 meV, more than two times larger than direct exchange for the case of cuprate holes in corner-sharing configuration of the ligand octahedra [32, 33]. How exactly SOC and Coulomb interactions commix to yield large anisotropic direct exchange integrals will be analyzed in detail elsewhere. The important point however is that, at the $t_{2g}^5 - t_{2g}^5$ SC level, there is a direct exchange matrix element for each possible pair of holes — $d_{xy} - d_{xy}$, $d_{xy} - d_{yz}$ etc. SOC mixes up those different Slater determinants, and the resulting spin-orbit wave-functions are not spin eigenstates. The ‘spin-orbit’ level structure can be reduced to an effective pseudospin model only by introducing anisotropic direct exchange matrix elements (i.e., the SC values provided in Table II).

Trigonal splittings in ‘213’ iridate structures. Spotting this particular RuCl_3 crystalline arrangement, where (i) the effects of ligand-cage trigonal compression and of farther-surrounding trigonal fields cancel out each other, (ii) the Ru-site t_{2g} levels are consequently degenerate (or nearly degenerate), such that close to ideal $j_{\text{eff}} = 1/2$ mo-

ments are realized, and (iii) the intersite isotropic Heisenberg interaction approaches zero, raises the question of whether an equivalent sweet spot can be identified in related Kitaev-Heisenberg quantum magnets, e.g. in Ir-oxide honeycomb compounds.

Interestingly, that the Heisenberg J changes its sign and therefore reaches a point where it simply vanishes has been already pointed out, for both ‘213’ hypothetical iridate structures [26] and $\text{H}_3\text{LiIr}_2\text{O}_6$ [27]. Such a situation is achieved in iridates for ligand-cage trigonal squeezing providing Ir-O-Ir bond angles of $\approx 98^\circ$ [26, 27] but an analysis of the on-site multiplet spectra was not performed in those specific iridate crystalline settings.

To verify this important aspect, we carried out additional quantum chemical computations for ‘iridate’ clusters having only one octahedron as central region, i.e., CASSCF calculations for a cluster consisting of one central IrO_6 octahedron and three adjacent octahedra in idealized Na_2IrO_3 setting with TM-ligand-TM bond angles of 98° [34]. The outcome of this numerical test is rewarding: also in the iridate system, a vanishing Heisenberg J [26] is associated with vanishing d -shell trigonal splittings, i.e., minor deviation from pristine $j_{\text{eff}} = 1/2$ states. In particular, without accounting for SOC, we find a trigonal splitting of only 25 meV within the Ir t_{2g} levels, to be compared with a spin-orbit coupling constant of 400–500 meV for Ir ions. That the near cancellation of ligand and ‘crystal’ trigonal fields occurs for stronger trigonal compression of the ligand cage ($\approx 98^\circ$ vs $\approx 93^\circ$ TM-ligand-TM bond angles) has to do with the larger effective charges in iridium oxides (formally, Ir^{4+} vs Ru^{3+} magnetic sites and O^{2-} vs Cl^- ligands). Notably, various Kitaev-Heisenberg superexchange models do assume (for simplicity) degenerate t_{2g} levels but not distorted TM-ligand-TM superexchange paths with bond angles away from 90° .

Conclusions. In spite of being central figure in nowadays research in quantum magnetism, textbook $j_{\text{eff}} = 1/2$ spin-orbit ground states [14] are rarely found in solids [35–37]. Here we show that nearly ideal $j_{\text{eff}} = 1/2$ moments are realized in a recently reported crystalline phase of RuCl_3 , identified under a pressure of 1.26 GPa [9]. In particular, we compute a vanishingly small trigonal splitting within the TM t_{2g} valence subshell in this crystallographic setting. Remarkably, this occurs in the presence of sizable trigonal squeezing of the ligand cages — it turns out that the effect of the latter is counterbalanced by trigonal fields having to do with the more distant crystalline surroundings. Moreover, the nearly ideal $j_{\text{eff}} = 1/2$ character of the pseudospins is associated with maximized K/J ratio for the intersite magnetic interactions, through a vanishingly small value of the nearest-neighbor Heisenberg J . The apparent correlation between these two features — neat $j_{\text{eff}} = 1/2$ moments and maximized K/J ratio — deserves careful further investigation, for instance, clarifying how different (super)exchange mech-

anisms cancel out each other for degenerate on-site t_{2g} orbital energies but nevertheless distorted TM-ligand-TM paths when it comes to isotropic exchange. Last but not least, we point out the important role of direct exchange [31] in the anisotropic spin interaction plot; curiously, direct exchange contributions have been so far neglected in K - J - Γ - Γ' exchange models.

Acknowledgments. P.B. and L.H. acknowledge financial support from the German Research Foundation (Deutsche Forschungsgemeinschaft, DFG), Project No. 441216021, and technical assistance from U. Nitzsche. Q.S. and J.G. thank the DFG (SFB 1143, project-id 247310070) and the Würzburg-Dresden Cluster of Excellence on Complexity and Topology in Quantum Matter-ct.qmat (EXC 2147, project-id 390858490) for financial support. We thank S. Nishimoto and G. Khaliullin for insightful discussions.

-
- [1] A. Kitaev, *Ann. Phys.* **321**, 2 (2006).
 - [2] G. Jackeli and G. Khaliullin, *Phys. Rev. Lett.* **102**, 017205 (2009).
 - [3] J. Chaloupka, G. Jackeli, and G. Khaliullin, *Phys. Rev. Lett.* **105**, 027204 (2010).
 - [4] H.-C. Jiang, Z.-C. Gu, X.-L. Qi, and S. Trebst, *Phys. Rev. B* **83**, 245104 (2011).
 - [5] A. Banerjee, C. A. Bridges, J.-Q. Yan, A. A. Aczel, L. Li, M. B. Stone, G. E. Granroth, M. D. Lumsden, Y. Yiu, J. Knolle, S. Bhattacharjee, D. L. Kovrizhin, R. Moessner, D. A. Tennant, D. G. Mandrus, and S. E. Nagler, *Nat. Mater.* **15**, 733 (2016).
 - [6] S.-H. Baek, S.-H. Do, K.-Y. Choi, Y. S. Kwon, A. U. B. Wolter, S. Nishimoto, J. van den Brink, and B. Büchner, *Phys. Rev. Lett.* **119**, 037201 (2017).
 - [7] Z. Wang, S. Reschke, D. Hivonen, S.-H. Do, K.-Y. Choi, M. Gensch, U. Nagel, T. Rößler, and A. Loidl, *Phys. Rev. Lett.* **119**, 227202 (2017).
 - [8] J. Zheng, K. Ran, T. Li, J. Wang, P. Wang, B. Liu, Z.-X. Liu, B. Normand, J. Wen, and W. Yu, *Phys. Rev. Lett.* **119**, 227208 (2017).
 - [9] Q. Stahl, T. Ritschel, G. Garbarino, F. Cova, A. Isaeva, T. Doert, and J. Geck, arXiv:2209.08367 (2022).
 - [10] R. Yadav, N. A. Bogdanov, V. M. Katukuri, S. Nishimoto, J. van den Brink, and L. Hozoi, *Sci. Rep.* **6**, 37925 (2016).
 - [11] S. M. Winter, Y. Li, H. O. Jeschke, and R. Valentí, *Phys. Rev. B* **93**, 214431 (2016).
 - [12] P. Warzanowski, N. Borgwardt, K. Hopfer, J. Attig, T. C. Koethe, P. Becker, V. Tsurkan, A. Loidl, M. Hermanns, P. H. M. van Loosdrecht, and M. Grüninger, *Phys. Rev. Res.* **2**, 042007 (2020).
 - [13] B. W. Lebert, S. Kim, V. Bisogni, I. Jarrige, A. M. Barbour, and Y.-J. Kim, *J. Phys.: Condens. Matter* **32**, 144001 (2020).
 - [14] A. Abragam and B. Bleaney, *Electron paramagnetic resonance of transition ions* (Clarendon Press, Oxford, 1970).
 - [15] H.-J. Werner, P. J. Knowles, G. Knizia, F. R. Manby, and M. Schütz, *WIREs Comput. Mol. Sci.* **2**, 242 (2012).

- [16] M. Klintonberg, S. Derenzo, and M. Weber, *Comp. Phys. Commun.* **131**, 120 (2000).
- [17] S. E. Derenzo, M. K. Klintonberg, and M. J. Weber, *J. Chem. Phys.* **112**, 2074 (2000).
- [18] T. Helgaker, P. Jørgensen, and J. Olsen, *Molecular Electronic Structure Theory* (John Wiley & Sons, Chichester, 2000).
- [19] D. A. Kreplin, P. J. Knowles, and H.-J. Werner, *J. Chem. Phys.* **152**, 074102 (2020).
- [20] P. J. Knowles and H.-J. Werner, *Theor. Chim. Acta* **84**, 95 (1992).
- [21] A. Berning, M. Schweizer, H.-J. Werner, P. J. Knowles, and P. Palmieri, *Mol. Phys.* **98**, 1823 (2000).
- [22] For the central Ru ion energy-consistent relativistic pseudopotentials (ECP28MDF) and Gaussian-type valence basis sets (BSs) of effective quadruple- ζ quality (referred to as ECP28MDF-VTZ in the MOLPRO library) [38] were employed, whereas we used all-electron triple- ζ BSs for the six Cl ligands of the central RuCl_6 octahedron [39]. The three adjacent TMs were represented as closed-shell $\text{Rh}^{3+} t_{2g}^6$ species, using relativistic pseudopotentials (Ru ECP28MDF) and (Ru ECP28MDF-VDZ) (4s4p3d)/[3s3p3d] BSs for electrons in the 4th shell [38]; the other 12 Cl ligands associated with the three adjacent TMs were described through minimal all-electron atomic-natural-orbital (ANO) BSs [40].
- [23] We employed relativistic pseudopotentials (ECP28MDF) and BSs (ECP28MDF-VTZ) as also used in the single-octahedron computations [38] for the central Ru species. All-electron BSs of quintuple- ζ quality were utilized for the two bridging ligands [39] and of triple- ζ quality for the remaining eight Cl anions [39] linked to the two octahedra of the reference unit. The four adjacent cations were represented as closed-shell $\text{Rh}^{3+} t_{2g}^6$ species, using the same pseudopotentials (Ru ECP28MDF) and BSs (Ru ECP28MDF-VDZ [3s3p3d]) [38] considered for the single-octahedron computations; the outer 16 Cl ligands associated with the four adjacent octahedra were described through minimal ANO BSs [40].
- [24] The t_{2g} orbitals of adjacent cations were part of the inactive orbital space.
- [25] N. A. Bogdanov, V. M. Katukuri, J. Romhányi, V. Yushankhai, V. Kataev, B. Büchner, J. van den Brink, and L. Hozoi, *Nat. Commun.* **6**, 7306 (2015).
- [26] S. Nishimoto, V. M. Katukuri, V. Yushankhai, H. Stoll, U. K. Rößler, L. Hozoi, I. Rousochatzakis, and J. van den Brink, *Nat. Commun.* **7**, 10273 (2016).
- [27] R. Yadav, M. S. Eldeeb, R. Ray, S. Aswartham, M. I. Sturza, S. Nishimoto, J. van den Brink, and L. Hozoi, *Chem. Sci.* **10**, 1866 (2019).
- [28] P. Bhattacharyya, N. A. Bogdanov, S. Nishimoto, S. D. Wilson, and L. Hozoi, arXiv:2212.09365 (2022).
- [29] N. A. Bogdanov, R. Maurice, I. Rousochatzakis, J. van den Brink, and L. Hozoi, *Phys. Rev. Lett.* **110**, 127206 (2013).
- [30] I. Rousochatzakis, J. Reuther, R. Thomale, S. Rachel, and N. B. Perkins, *Phys. Rev. X* **5**, 041035 (2015).
- [31] P. W. Anderson, *Phys. Rev.* **115**, 2 (1959).
- [32] R. L. Martin, *J. Chem. Phys.* **98**, 8691 (1993).
- [33] A. van Oosten, R. Broer, and W. Nieuwpoort, *Chem. Phys. Lett.* **257**, 207 (1996).
- [34] For the central Ir ion relativistic pseudopotentials (ECP60MDF) and BSs of effective quadruple- ζ quality (ECP60MDF-VTZ) [41] were used, whereas we applied all-electron triple- ζ BSs [42] for the six O ligands of the central IrO_6 octahedron. The three adjacent TMs were represented as closed-shell $\text{Pt}^{4+} t_{2g}^6$ species, using relativistic pseudopotentials (Ir ECP60MDF) and (Ir ECP60MDF-VDZ) (4s4p3d)/[3s3p3d] BSs [41]. The other 12 O ligands associated with the three adjacent TM sites were described through minimal all-electron ANO BSs [40]. Large-core pseudopotentials were employed for the 18 adjacent Na cations [43].
- [35] A. Revelli, C. C. Loo, D. Kiese, P. Becker, T. Fröhlich, T. Lorenz, M. Moretti-Sala, G. Monaco, F. L. Buessen, J. Attig, M. Hermanns, S. V. Streltsov, D. I. Khomskii, J. van den Brink, M. Braden, P. H. M. van Loosdrecht, S. Trebst, A. Paramekanti, and M. Grüninger, *Phys. Rev. B* **100**, 085139 (2019).
- [36] D. Reig-i Plessis, T. A. Johnson, K. Lu, Q. Chen, J. P. C. Ruff, M. H. Upton, T. J. Williams, S. Calder, H. D. Zhou, J. P. Clancy, A. A. Aczel, and G. J. MacDougall, *Phys. Rev. Materials* **4**, 124407 (2020).
- [37] N. Khan, D. Prishchenko, M. H. Upton, V. G. Mazurenko, and A. A. Tsirlin, *Phys. Rev. B* **103**, 125158 (2021).
- [38] K. A. Peterson, D. Figgen, M. Dolg, and H. Stoll, *J. Chem. Phys.* **126**, 124101 (2007).
- [39] D. E. Woon and T. H. Dunning Jr., *J. Chem. Phys.* **98**, 1358 (1993).
- [40] K. Pierloot, B. Dumez, P.-O. Widmark, and B. O. Roos, *Theor. Chim. Acta* **90**, 87 (1995).
- [41] D. Figgen, K. A. Peterson, M. Dolg, and H. Stoll, *J. Chem. Phys.* **130**, 164108 (2009).
- [42] T. H. Dunning, *J. Chem. Phys.* **90**, 1007 (1989).
- [43] P. Fuentealba, H. Preuss, H. Stoll, and L. Von Szentpály, *Chem. Phys. Lett.* **89**, 418 (1982).